



Geofísica Internacional

ISSN: 0016-7169

silvia@geofisica.unam.mx

Universidad Nacional Autónoma de México
México

Valenzuela, Raúl W.; Galindo, Marta; Pacheco, Javier F.; Iglesias, Arturo; Terán, Luis F.; Barreda, José L.; Coba, Carlos
Seismic survey in southeastern Socorro Island: Background noise measurements, seismic events, and T phases
Geofísica Internacional, vol. 44, núm. 1, january-march, 2005, pp. 23-38
Universidad Nacional Autónoma de México
Distrito Federal, México

Available in: <http://www.redalyc.org/articulo.oa?id=56844103>

- How to cite
- Complete issue
- More information about this article
- Journal's homepage in redalyc.org

redalyc.org

Scientific Information System
Network of Scientific Journals from Latin America, the Caribbean, Spain and Portugal
Non-profit academic project, developed under the open access initiative

Seismic survey in southeastern Socorro Island: Background noise measurements, seismic events, and T phases

Raúl W. Valenzuela¹, Marta Galindo², Javier F. Pacheco¹, Arturo Iglesias¹, Luis F. Terán¹, José L. Barreda³ and Carlos Coba³

¹ *Instituto de Geofísica, Universidad Nacional Autónoma de México, Mexico City, Mexico*

² *Comprehensive Nuclear-Test-Ban Treaty Organization, IMS, Vienna, Austria*

³ *Facultad de Ingeniería, Benemérita Universidad Autónoma de Puebla, Puebla City, Mexico*

Received: July 16, 2003; accepted: December 5, 2003

RESUMEN

En junio de 1999 instalamos cinco sismómetros portátiles de banda ancha en el sureste de la Isla Socorro. Se encontró que las densidades espectrales de potencia en los cinco sitios son relativamente ruidosas en comparación con las curvas mundiales de referencia. Este resultado concuerda con observaciones realizadas en otras islas pequeñas. Las densidades espectrales de potencia permanecen constantes sin importar la hora del día o el día de la semana. Los efectos del ruido cultural en la isla son muy pequeños. Se identificaron los sitios con el mayor y el menor ruido. Esta información servirá para determinar la ubicación de la estación de fase T que será instalada conjuntamente por la Universidad Nacional Autónoma de México y la Organización del Tratado para la Prohibición Completa de Ensayos Nucleares. Durante el periodo de estudio se registraron seis sismos. Estos ocurrieron a distancias epicentrales entre 42 y 2202 km y tuvieron magnitudes entre 2.8 y 7.0. Dos sismos pequeños ($M_c = 2.8$ y 3.3) y cercanos ocurrieron en la Zona de Fractura de Clarión. Los cuatro eventos más grandes y más lejanos generaron ondas T . La onda T producida por un temblor cerca de la costa de Guatemala tuvo una duración de alrededor de 100 s y frecuencias entre 2 y 8 Hz, con un máximo en su amplitud aproximadamente a 4.75 Hz. El terremoto de Tehuacán del 15 de junio de 1999 ($M_w = 7.0$) generó ondas $P \rightarrow T$ y $S \rightarrow T$, ambas con energía entre 2 y 3.75 Hz. Dicho sismo ocurrió dentro de la placa subducida de Cocos a una profundidad de 60 km y el epicentro se localizó lejos de la costa del océano Pacífico. Esto implica que un segmento largo de la trayectoria fue recorrido por tierra. Inicialmente la energía viajó en forma de ondas sísmicas P y S , las cuales probablemente se propagaron por dentro de la placa subducida, y éstas después se convirtieron a energía acústica al pasar de la tierra al agua en el talud continental frente a la costa del océano Pacífico. La duración total de la fase T es cercana a los 500 s y alcanza su amplitud máxima alrededor de 200 s después de la llegada de la onda $P \rightarrow T$. La fase T tiene energía en frecuencias entre 2 y 10 Hz y alcanza su amplitud máxima a aproximadamente 2.5 Hz. También se registraron las fases T producidas por un sismo en el estado de Guerrero, México y otro en la Zona de Fractura de Rivera.

PALABRAS CLAVE: Tratado para la Prohibición Completa de Ensayos Nucleares (TPCEN), canal de fijación y determinación de la distancia por sonido (SOFAR), explosiones nucleares, Isla Socorro, fases T , Zona de Fractura de Clarión, Zona de Fractura de Rivera, océano Pacífico.

ABSTRACT

We carried out a seismic survey and installed five portable, broadband seismometers in the southeastern corner of Socorro Island during June 1999. Power spectral densities for all five sites were relatively noisy when compared to reference curves around the world. Power spectral densities remain constant regardless of the time of day, or the day of the week. Cultural noise at the island is very small. Quiet and noisy sites were identified to determine the best location of the T phase station to be installed jointly by the Universidad Nacional Autónoma de México and the Comprehensive Nuclear-Test-Ban Treaty Organization. During the survey six earthquakes were recorded at epicentral distances between 42 km and 2202 km, with magnitudes between 2.8 and 7.0. Two small earthquakes ($M_c = 2.8$ and 3.3) occurred on the Clarión Fracture Zone. The four largest and more distant earthquakes produced T waves. One T wave from an epicenter near the coast of Guatemala had a duration of about 100 s and a frequency content between 2 and 8 Hz, with maximum amplitude at about 4.75 Hz. The Tehuacán earthquake of June 15, 1999 ($M_w = 7.0$) produced arrivals of $P \rightarrow T$ and $S \rightarrow T$ waves, with energy between 2 Hz and 3.75 Hz. The earthquake occurred inland within the subducted Cocos plate at a depth of 60 km; a significant portion of the path was continental. Seismic P and S waves probably propagated upward in the subducted slab, and were converted to acoustic energy at the continental slope. Total duration of the T phase is close to 500 s and reaches its maximum amplitude about 200 s after the $P \rightarrow T$ arrival. The T wave contains energy at frequencies between 2 and 10 Hz and reaches its maximum amplitude at about 2.5 Hz. T phases were also recorded from two earthquakes in Guerrero, Mexico and in the Rivera Fracture Zone.

KEY WORDS: Comprehensive Nuclear-Test-Ban Treaty (CTBT), Sound Fixing and Ranging (SOFAR) channel, nuclear explosions, Socorro Island, T phases, Clarión Fracture Zone, Rivera Fracture Zone, Pacific ocean.

1. INTRODUCTION

The Comprehensive Nuclear-Test-Ban Treaty (CTBT) bans all nuclear explosions above ground, underwater, and underground, whether for military or civilian purposes. One of the main components of the Comprehensive Nuclear-Test-Ban Treaty Organization (CTBTO), headquartered in Vienna, is the International Monitoring System (IMS). The IMS is currently deploying a global network aimed to guarantee compliance with the treaty. This network relies on four different technologies (Sullivan, 1998). Seismic, hydroacoustic, and infrasound stations are used to record waves from underground, submarine, and atmospheric explosions. Radionuclide stations can detect radioactive isotopes produced by atmospheric explosions as well as isotopes that leak into the atmosphere from underground or underwater explosions.

Mexico signed the treaty on September 24, 1996 and ratified it on October 5, 1999. Five IMS stations are to be located in Mexico. The operation of a radionuclide station has been assigned to the Comisión Nacional de Seguridad Nuclear y Salvaguardias (National Commission for Nuclear Safety and Safeguard) while three auxiliary seismic stations and one *T* phase station were assigned to the Servicio Sismológico Nacional (SSN) at the Instituto de Geofísica of the Universidad Nacional Autónoma de México (National Seismology Bureau at the Institute of Geophysics of the Mexican National University).

The Hydroacoustic Monitoring Section of the IMS is concerned with the detection of acoustic energy from potential nuclear explosions in the oceans. Due to conditions of salinity and temperature, there exists a low velocity layer in the oceans' water. The sound velocity decreases from the sea surface down to depths between 600 and 1800 m (Okal, 2001), where it reaches a minimum of about 1.5 km/s (Kulhánek, 1990). From this depth down to the bottom, the sound velocity increases again. This low velocity region is called the Sound Fixing And Ranging (SOFAR) channel and it allows for the efficient propagation of high frequency (greater than 2.5 Hz) sound waves (Okal, 2001). The IMS uses two different technologies to detect acoustic energy that has propagated in the ocean. The first method relies on the deployment of hydrophones within the SOFAR channel (Sullivan, 1998; Newton and Galindo, 2001). The second one is based on the conversion of a hydroacoustic wave into seismic waves upon striking an island or continent (Sullivan, 1998; Okal, 2001; Newton and Galindo, 2001). The seismic energy may be transmitted through the land portion of the path as a *P*, *S*, or surface wave and is in general designated as a *T* wave (Kulhánek, 1990). *T* stands for tertiary wave because on a seismogram it arrives after the *P* (primary) and *S* (secondary) waves (Kulhánek, 1990). *T* waves were observed as early as 1927 (Okal, 2001). CTBTO's hydroacoustic network will be made up of six underwater hydrophone stations

and five island-based *T* phase stations (Sullivan, 1998; Newton and Galindo, 2001). A *T* phase station can be built using a short period or a broadband seismometer operating at a sufficiently high sampling rate (50 to 100 samples per second). While the *T* phase stations are not as sensitive as the hydrophone stations, their construction, operation and maintenance is simpler and thus have a lower cost (Sullivan, 1998; Newton and Galindo, 2001).

Given the efficient propagation of the high frequency hydroacoustic waves through the SOFAR channel, *T* waves are easy to detect (Talandier and Okal, 1998) and have been recorded at epicentral distances as far away as 83° (Kulhánek, 1990). Under very favorable conditions *T* phases have even been felt by people several thousand kilometers from the source (Talandier and Okal, 1979). These acoustic waves travel through the water at a relatively slow speed, which leads to a good precision for the location of sources based on *T* wave arrival times (Talandier and Okal, 1998). This combination of good detection and location makes *T* waves a useful tool for the monitoring and identification of small sources in remote areas.

The Mexican *T* phase station will be built in Socorro Island, Revillagigedo Archipelago (Figure 1). A site survey was conducted jointly by the SSN and the CTBTO in June 1999 in order to determine the best location for the station. Five seismometers were installed in the southeast corner of the island and measured the levels of background noise. During the survey six earthquakes were recorded at epicentral distances between 42 and 2202 km. Their magnitudes ranged between 2.8 and 7.0. The four largest events generated *T* phases.

2. DESCRIPTION OF THE SURVEY

Socorro Island belongs to the Revillagigedo Archipelago and is located at approximately 18.8° N, 111.0° W in the eastern Pacific ocean (Figure 1). The island has an elongate NW-SE shape with maximum dimensions of about 15 km × 15 km in the N-S and E W directions. It is located about 700 km west of the port of Manzanillo, Colima state. Socorro represents the emergent peak of a large basaltic shield volcano that rises from a sea floor depth of ~3000 m. Its highest elevation is Mount Evermann at 1050 m a. m. s. l. The island's average submarine slope is a little less than 10° (Siebe *et al.*, 1995). Socorro was chosen by the CTBTO to provide coverage of the east-central Pacific (Newton and Galindo, 2001). We operated five temporary, portable broadband stations at the island in June 1999. The first seismometer (SBNA) was installed on the pier inside the existing building of a seismic station that was built by Mexico's Servicio Sismológico Nacional and the Mexican Navy just outside the navy's village (Figure 1). This SSN station is no longer operational. Temporary station SBNA operated the

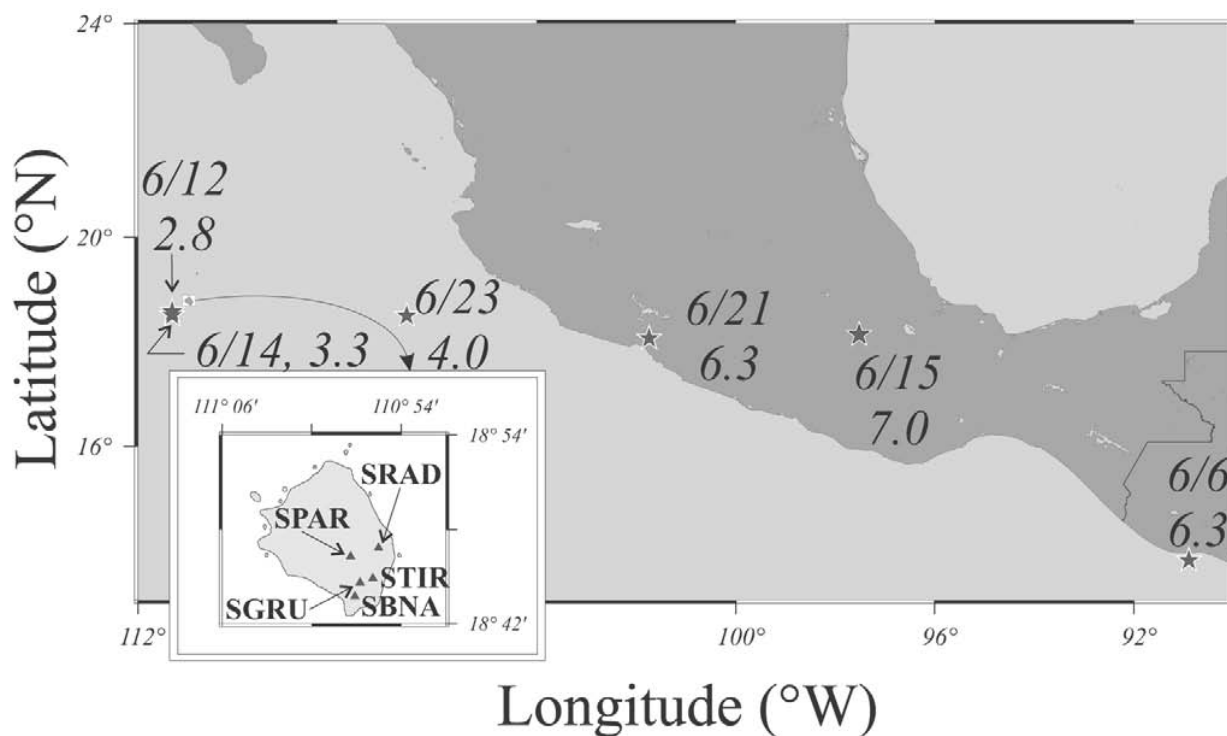


Fig. 1. Location of Socorro Island relative to the Mexican mainland. The inset shows the island. The triangles mark the locations of the five stations deployed in the southeastern quadrant. The stars are the epicenters of the events recorded during June 1999. The first number associated with each earthquake is the date. The second number is the magnitude.

longest due to its accessibility. It recorded during the period from June 6 through June 24 (UTC), 1999. All five stations operated simultaneously for close to nine consecutive days, during the period from June 8 through June 17. The location of all five seismometers is shown in Figure 1 and their coordinates are listed in Table 1. These coordinates were averaged from the readings recorded by the data acquisition system every time its Global Positioning System (GPS) clock locked. The elevations reported in Table 1 were read directly from a topographic map (Dirección General de Geografía, 1992). We feel that this method gives a smaller error than using the GPS determined elevation because of the large vertical errors associated with these measurements. There is a dirt road linking the navy village and the landing strip. Given that this is virtually the only road on Socorro, work was constrained to the southeastern corner of the island. Access to other locations throughout the island is rather difficult, especially if equipment has to be transported.

We installed three-component, broadband CMG-40T Güralp velocity seismometers. The bandpass for these instruments ranges from 30 s to 50 Hz. We used RefTek 72A-07 data acquisition systems and stored the data on hard disks. The data were recorded in continuous mode at a sampling rate of 100 sps. The data segment length was 30 minutes at all sites except at SGRU, where a segment length of 25 min-

utes was used for the first few days. Timing was achieved through GPS clocks. Power was supplied through two car batteries which were recharged using one solar panel at each of the four sites outside the village. For the instrument installed in the village, power was fed from a regular AC outlet (through an AC/DC converter). The stations were built following the standard practice for installing portable seismic stations for a period of several weeks. In order to minimize the effects of temperature changes and also to better protect the seismometers, the four instruments installed in the field were buried inside holes 50 to 90 cm deep. These instruments were placed inside plastic bags so that they would be protected from moisture and dirt. Putting the sensors on a tile fixed to the ground with some mortar made it easier to level them. It was not possible to bond the tile to a rock for better stability and coupling of the instrument because no suitable rocks were found at the appropriate depths. Once the instruments were leveled, a plastic bucket was placed over them and they were buried and covered by a small mound afterwards.

3. ANALYSIS OF SEISMIC BACKGROUND NOISE

Data were recorded simultaneously at all five stations for a total of ~8.5 days. The spectra were calculated using this time period, which runs from Julian day 160 at 00:00

Table 1

Locations of the seismic stations on Socorro Island, June 1999

Station Code	RefTek S/N	Güralp S/N	Latitude	Longitude	Elevation (m)	Location
SBNA	7381	T4289	18° 43.746' N	110° 57.116' W	60	Navy village
SGRU	7548	T4273	18° 44.628' N	110° 56.765' W	175	Near the caves
STIR	7184	T4471	18° 44.905' N	110° 55.910' W	260	Shooting range
SPAR	7549	T4474	18° 46.301' N	110° 57.387' W	510	Road to volcano's summit
SRAD	7547	T4473	18° 46.844' N	110° 55.505' W	300	Radar station

UTC to day 168 shortly after 14:00 UTC. In order to assess the effects of cultural noise depending on the time of day, each day was divided into four 6-hour blocks and then two 5 minute segments per block were simultaneously extracted from all five stations. The blocks range from 00:00 to 06:00, from 06:00 to 12:00, and so on, using local time. On any one day, the 5-minute segments were chosen 3 hours apart from each other. For example, on day 160 the first segment was chosen at 00:00, the second at 03:00, then at 06:00 and so on. For the following day, the segments were chosen one hour later than the day before, that is, on day 161 the segments were selected at 01:00, 04:00, 07:00 and so on. We conducted a visual check of all the 5-minute segments in order to avoid contamination from particular events as well as other potential problems with data quality. The 5-minute segments were processed using the Seismic Analysis Code (SAC) and were both demeaned and detrended to avoid any contamination of the spectra. The power spectral estimate was calculated using program `pspecsac.f` (L. Astiz, Comprehensive Nuclear-Test-Ban Treaty Organization, personal communication, 1999). The power spectral density was subsequently obtained from the power spectral estimate (J. Pacheco, Universidad Nacional Autónoma de México, unpublished, 2000). For any given station we averaged all the 5-minute segments (from all ~8.5 days) corresponding to each of the four 6-hour blocks. No significant effect from cultural noise (except for the electricity generators at SBNA, as explained below) was observed and the power spectral densities remain essentially constant regardless of the time of day, or the day of the week. This result was expected because the population of the island is small (less than 100 persons). Figure 2 compares the power spectral density of all the stations for a given component (Z, N, or E) on June 16, 1999 at 9:00 UTC and is considered representative of the noise levels at the different locations. This time window was chosen at random. The plots in Figure 2 were obtained using the SPEC program from the SEISAN package, which allows for the deconvolution of the seismometer's instrument response as well as the digitizer from the velocity records. Reference

curves for high and low-noise sites around the world are also shown in Figure 2. The noise levels for all five sites at the island are greater than the middle of the range defined by these high and low-noise reference curves. Sites on small islands around the world are generally noisy. When looking at the power spectral density curves in Figure 2 it is important to remember that the bandpass for the CMG-40T Güralp velocity sensor runs from 0.0333 to 50 Hz and that a sampling rate of 100 sps was used (appropriate for a Nyquist frequency at 50 Hz).

In general, Figure 2 shows that the level of noise on the vertical component for all stations is lower than for their respective horizontal components. The power spectral density curves for the vertical component for all five stations are very similar in the frequency range between 0.1 and 1 Hz. Likewise, the power spectral density curves for each of the two horizontal components (N-S and E-W) are very similar for all five stations but in a narrower frequency range, from 0.1 to 0.5 Hz. Some differences in the vertical component power spectral density curves exist for the various stations at frequencies higher than 1 Hz, and at frequencies above 0.5 Hz for the horizontal components. SRAD and SPAR are the two most quiet sites at the frequencies of interest for the detection of earthquake-generated *T* waves (between 2 and 10 Hz) while STIR is the noisiest. *T* waves generated by volcanic activity or by man-made explosions could be recorded at higher frequencies if the path from the shore to the seismometer is short enough that it will not attenuate them.

A simple visual inspection of the time domain records from station SBNA reveals a considerable content of high frequency noise. The source of the noise was traced to the diesel generators used to produce electricity for the village. Figure 2 shows a clear spike reaching about -70 dB around 30 Hz frequency. Even though the strongest effect is observed at ~30 Hz, noise can be significant at frequencies between 10 and 50 Hz.

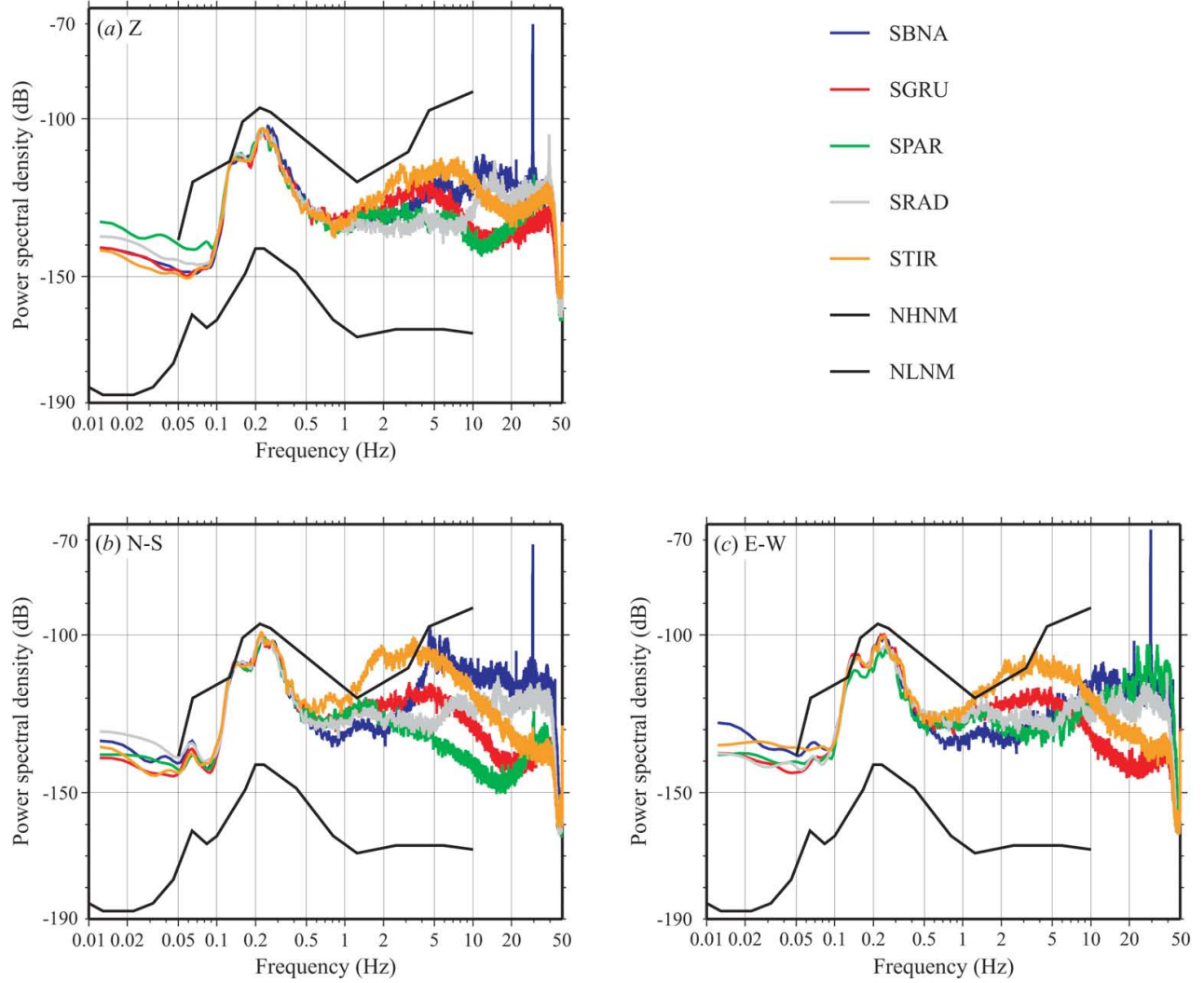


Fig. 2. Power spectral densities by component (Z, N, E) for all five stations on June 16, 1999 at 9:00 UTC. This example was chosen at random and is considered representative of the noise levels at the different locations regardless of the time of day, or the day of the week. These plots were calculated using the SPEC program from SEISAN which deconvolved the effects of the seismometer's instrument response and the digitizer from the velocity records. Average USGS curves from high and low-noise sites around the world are shown for reference.

4. SEISMIC EVENTS RECORDED AT SOCORRO ISLAND

During the time of the deployment (June 6 to 24, 1999) six different earthquakes were recorded on at least one station. Figure 1 shows their epicenters. All five stations operated simultaneously for close to nine consecutive days starting on Julian day 159 (June 8) and ending on day 168 (June 17). The station installed in the village (SBNA) operated the longest given that it was the most easily accessible. It operated between days 157 (June 6) and 175 (June 24) and therefore recorded all six events. Three earthquakes were recorded by all five stations. Table 2 summarizes the six events giving

their date, origin time, hypocenter, magnitude, epicentral distance to station SBNA, number of stations which produced a record, and the geographical location. The parameters presented in Table 2 are the best ones available. For example, the earthquake of Tehuacán, Puebla state, Mexico was the most extensively studied (Singh *et al.*, 1999) due to its location and magnitude. We determined the source parameters for the events on the Clarión Fracture Zone given that they were not recorded anywhere else. For the events near the coast of Guatemala, in Guerrero state, Mexico, and on the Rivera Fracture Zone, information from the International Seismological Centre (1999) was used. The earthquakes in Tehuacán, in Guerrero state, and on the Rivera Fracture Zone

Table 2

List of events recorded on Socorro Island between June 6 and 24, 1999

Date Y/M/D	Origin time H:M:S	Lat. (°N)	Long. (°W)	Depth (km)	Mag. ^a	Distance ^b (km)	No. Stat. ^c	Location	Source ^d
99/06/06	07:08:12	13.93	90.91	86	6.3 M_w	2202	1	Near coast of Guatemala	A
99/06/12	06:06:06	18.59	111.32	1	2.8 M_c	42	5	Clarión Fracture Zone	B
99/06/14	10:33:02	18.52	111.31	1	3.3 M_c	44	5	Clarión Fracture Zone	B
99/06/15	20:42:05	18.15	97.52	60	7.0 M_w	1419	5	Tehuacán, Puebla, México	C
99/06/21	17:43:06	18.44	101.54	78	6.3 M_w	993	1	Guerrero, México	A
99/06/23	00:58:28	18.70	106.40	20	4.0 m_b	480	1	Rivera Fracture Zone	D

^a Magnitude: M_w = moment magnitude; M_c = coda magnitude; m_b = body wave magnitude.^b Epicentral distance to station SBNA.^c Number of stations that recorded the event. When only one station recorded the event, this was SBNA.^d Source of the parameters listed:

A - All parameters from the International Seismological Centre (ISC, 1999), except for the magnitude which was taken from the Harvard catalog as reprinted in the ISC Bulletin.

B - This study. The depth was constrained to 1 km for the location procedure.

C - Origin time from the International Seismological Centre (1999); all other parameters from Singh *et al.* (1999).

D - International Seismological Centre (1999).

were also reported by Mexico's Servicio Sismológico Nacional. The events recorded have epicentral distances between 42 km (Clarión FZ) and 2202 km (near coast of Guatemala). Their range of magnitudes goes from $M_c=2.8$ (Clarión FZ) to $M_w=7.0$ (Tehuacán). Some observations concerning the different events recorded are presented below.

06/06/1999 Near coast of Guatemala.- This earthquake ($M_w = 6.3$) was only recorded by station SBNA, at an epicentral distance of 19.81° (2202 km). The record shows both, clear *P* and *S* arrivals. The N-S velocity record is shown in Figure 3a.

06/12 and 14/1999 Clarión Fracture Zone (CFZ).- These two events were recorded by all five stations and have *S-P* times of about 6 or 7 seconds. The distance to the stations is approximately 45 km. The coda magnitudes are 2.8 and 3.3 for the 6/12 and the 6/14 events, respectively. Given that these two events were only recorded by our stations, we located the events ourselves using both *P* and *S* arrival times. The general *iasp91* travel time tables (Kennett and Engdahl, 1991) were used and the depth was constrained at 1 km in order to make the location procedure stable. The epicenters were plotted on a bathymetric map of the area (Dirección General de Geografía, 1988) and they located southwest of Socorro Island and slightly north of the Clarión FZ. While we do not rule out the possibility that the events occurred north of the fracture, we consider it more likely that they indeed are located on the CFZ given (1) the uncertainty in-

herent to all location procedures, (2) the lack of a local seismic velocity model for the crust and mantle, (3) the errors associated with the maps and the poorly known bathymetry, (4) the poor station geometry (the events are outside of the network), and (5) the higher seismicity expected for a fracture zone. The magnitude was calculated from the coda duration.

06/15/1999 Tehuacán, Puebla state, Mexico.- This event ($M_w = 7.0$) was recorded by all five stations. The epicentral distance to station SBNA is 12.76° (1419 km). The records clearly show the *P* and *sP* arrivals and surface waves. Figure 4a shows the velocity records from station SRAD.

06/21/1999 Guerrero state, Mexico.- The earthquake ($M_w=6.3$) was recorded only by station SBNA, at an epicentral distance of 8.93° (993 km). The *S* arrival and the surface waves show clearly. The *P* wave pick is very dubious.

06/23/1999 Rivera Fracture Zone.- This event ($m_b = 4.0$) was recorded only by station SBNA, at an epicentral distance of 4.31° (480 km). The records show clear *S* and surface waves but the *P* arrival is questionable.

Perhaps the most interesting result was the detection of small events that occurred on the Clarión Fracture Zone, about 45 km southwest of the island. Once CTBTO's *T* phase station is built on Socorro Island, it should be possible to detect

seismic activity associated to the nearby fracture zones (Rivera, Clarión, Orozco, O’Gorman, Clipperton, and Siqueiros FZs) and also associated to the volcanoes on both Socorro and San Benedicto islands. At the time of the most recent volcanic activity at Socorro Island in 1993, Navy personnel reported feeling earthquakes (Siebe *et al.*, 1995). Bárcena volcano was born in 1952 on San Benedicto Island, about 50 km NNE from Socorro Island (Siebe *et al.*, 1995).

5. *T* WAVES RECORDED AT SOCORRO ISLAND

Initially, the epicentral distances for the events in Table 2 were divided by 1.48 km/s, *i. e.* the velocity of the *T* wave in the SOFAR channel in the Pacific ocean (Talandier and Okal, 1998), in order to obtain the *T* wave travel times. We determined an approximate arrival time and looked at the seismograms for any indications that *T* waves had been recorded. Given that *T* waves carry their energy at high frequencies, the seismograms were filtered to enhance the signal at frequencies above 2 Hz. *T* phases were observed for the four largest earthquakes recorded. Once the *T* waves were identified, the calculation of the expected arrival time was improved. The travel time was determined from the propagation of a seismic wave (either *P* or *S*) through land plus the propagation of an acoustic wave through water.

Additionally, during the period from June 9th through the 16th, when all five seismometers operated simultaneously, the records were bandpass filtered between 2 and 20 Hz. The signals from all the stations were compared in an attempt to identify the arrival of *T* waves from small or distant events whose body or surface waves were not recorded by the seismometers. Potential *T* phases were singled out from several seismograms. After checking the CTBTO’s International Data Center Revised Event Bulletin, *T* waves could be associated with five more earthquakes.

T phase observations for the event of 06/06/1999 Near coast of Guatemala.- At the time of this earthquake, only station SBNA had been installed. The unfiltered N-S component for this earthquake shows a *T* phase at about 07:32:30 (Figure 3a). As previously explained, this station is very noisy at frequencies greater than 10 Hz. For this reason the records were bandpass filtered between 1 and 10 Hz. Figure 3b shows an even earlier *T* wave arrival at about 07:31:47 in all three components. A second packet of energy is observed at about 07:32:26 and has a greater amplitude than the earlier arrival (Figure 3b). This is the wave previously observed in the unfiltered seismograms. The total duration of these two packets combined is on the order of 100 s.

The spectrogram for the bandpass filtered N-S component was calculated using the Seismic Analysis Code (SAC), see Figure 3c. It shows that the energy for the first arrival is concentrated at frequencies between 3 and 7 Hz with a maxi-

mum at about 4.75 Hz. The energy for the second, larger wave has a frequency contents between 2 and 8 Hz and reaches its maximum at about 4.75 Hz.

The expected arrival time at SBNA was calculated assuming that the conversion from seismic to acoustic energy occurs on the great circle path, about 1.21° (or 135 km) from the epicenter. The coordinates for this point are roughly at 14.3°N, 92.1°W, offshore and south of the border between Chiapas state and Guatemala. However, it was not possible to determine the exact location of the conversion point on the continental slope, as the coordinates listed correspond to a region of shallow bathymetry (Dirección General de Geografía, 2000) and coupling into the SOFAR channel seems unlikely. The distance from the point used for the calculation to the station is 18.60° (2068 km). The travel time for the *P* wave to the assumed conversion point is 22 s and for the *S* wave is 39 s. Taking a velocity of 1.48 km/s (Talandier and Okal, 1998), the acoustic wave has a travel time of 1397 s. Therefore, the estimated arrival time for the *P* → *T* wave is 07:31:51 and 07:32:08 for the *S* → *T* wave. The observed arrival time is 07:31:47. Calculations choosing a seismic-to-acoustic transition point farther west, placed on the 1000-m depth contour, resulted in an arrival time which is early by about 110 s.

T phase observations for the event of 06/15/1999 Tehuacán, Puebla state, Mexico.- This earthquake was recorded by all five stations. Unlike the Guatemala event, the *T* waves from this earthquake are not seen on the unfiltered seismograms. After highpass filtering the records at 2 Hz, all three components show the arrival of the *T* wave at about 20:53:06 at station SRAD (Figure 4b). Nonetheless, the *T* wave reaches its maximum amplitude about 150 s later (Figure 4b). In fact, Figure 4b shows that the energy from the *T* wave lasts for at least 400 s. The backazimuth at this station is $\phi_b = 90.7^\circ$. Therefore, the N-S component can essentially be treated as the transverse component. Likewise, the E-W component is very close to the radial.

Calculation of the spectrogram for the filtered N-S component reveals an even earlier arrival at about 20:51:59 and brings the total duration of the *T* wave close to 500 s (Figure 4c). Figures 4a and 4b show that the *T* wave is weak by comparison to the coda. Even though the coda has most of its energy at frequencies below 2 Hz, it became necessary to filter the seismograms so that the *T* wave could be seen in the spectrogram. The spectrogram shows that the energy of the *T* wave is concentrated at frequencies between 2 and 10 Hz with a maximum at about 2.5 Hz (Figure 4c). The two packets of energy for which arrival times were obtained have frequencies below 4 Hz (Figure 4c).

This is an intermediate depth, in-slab earthquake and its epicenter is not anywhere near the shore. Therefore, the

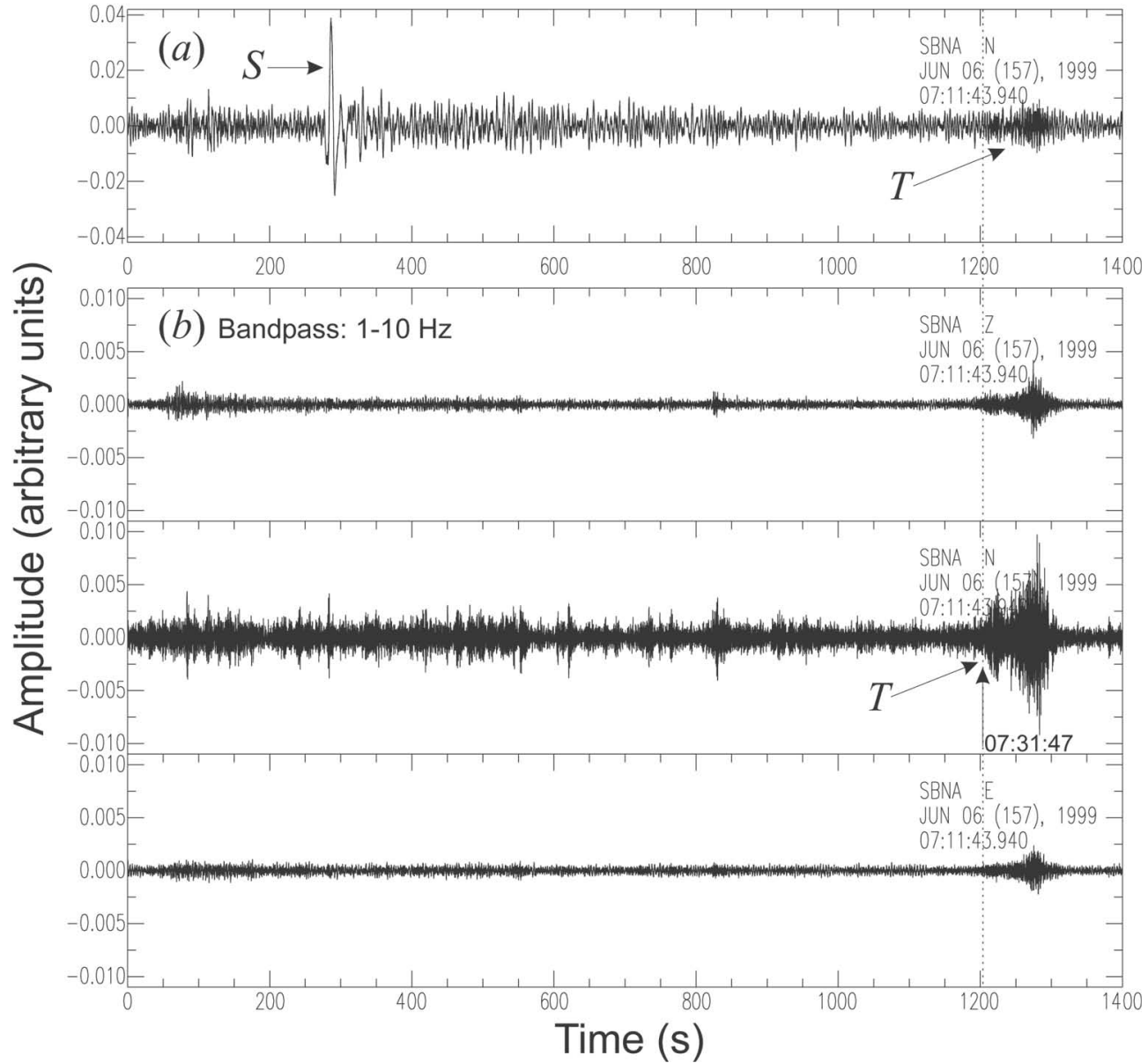


Fig. 3. Velocity records for the event near the coast of Guatemala, 06/06/1999, at station SBNA. (a) unfiltered time series for the N-S component. The *S* and *T* arrivals are indicated. (b) the time series were bandpass filtered between 1 and 10 Hz in order to enhance the *T* phase. The vertical arrow points to the observed “arrival” time of the *T* wave. The three components are shown at the same scale.

propagation of a seismic wave through land plus the propagation of an acoustic wave through water had to be taken into account in order to calculate the estimated arrival time of the *T* wave at the station. We looked at the great circle path on a hypsographic map (Dirección General de Geografía, 2000) and estimated that the conversion of seismic-to-acoustic energy occurs on the continental slope, off the west coast of Mexico, at approximately 18.5°N, 104.0°W, corresponding to an ocean depth of ~1000 m. Thus, the distance be-

tween the epicenter and the seismic-to-acoustic transition point is 6.16° (or 685 km) while the distance between the transition point and station SRAD is 6.57° (731 km). Since the seismic energy can propagate from the epicenter to the transition point either as a *P* or an *S* wave, both travel times were calculated. The travel time for the *P* wave is 88 s and for the *S* wave is 158 s. For a distance of 731 km between the continental slope and the seismic station, the travel time for the acoustic wave, propagating at 1.48 km/s (Talandier and

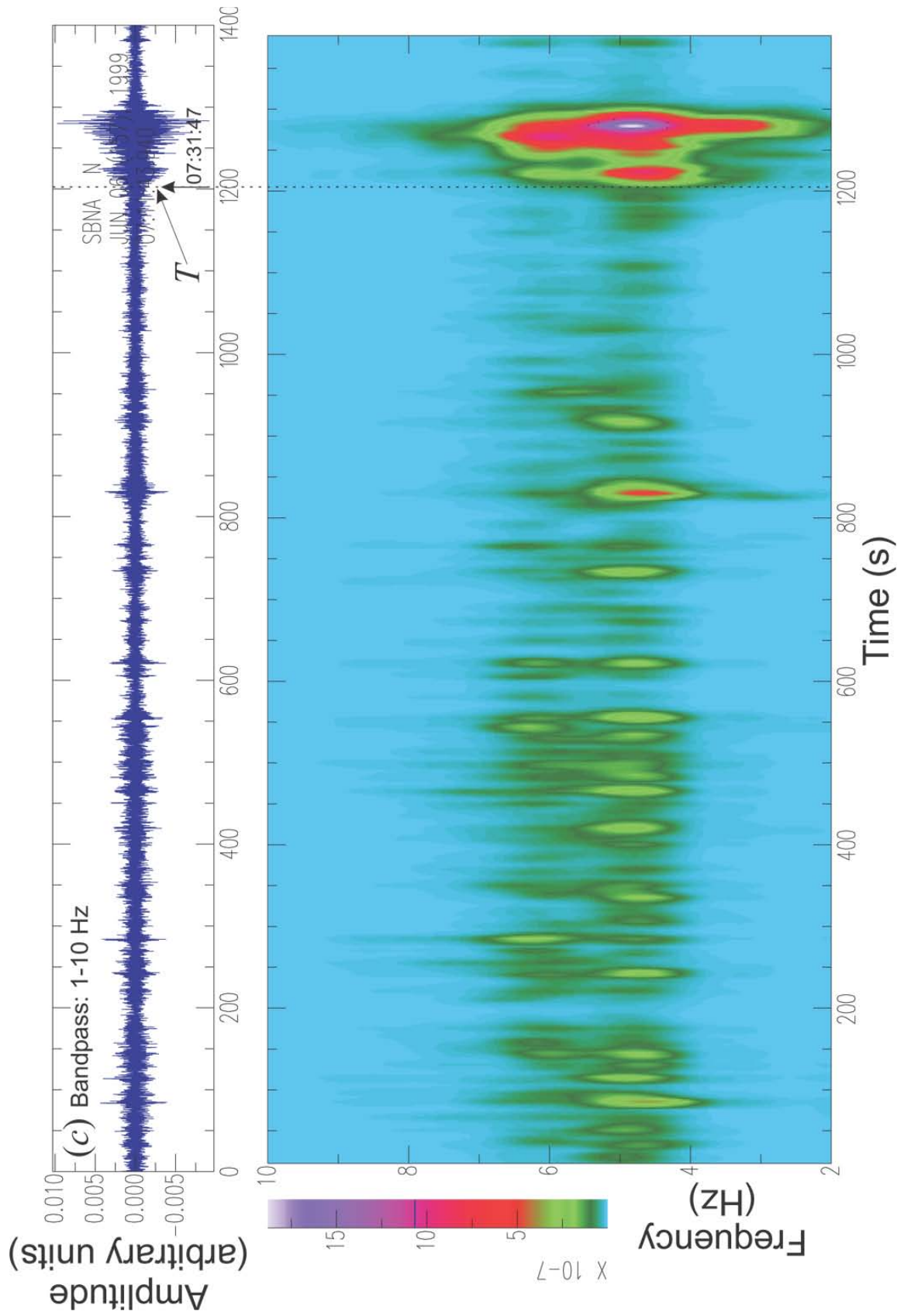


Fig. 3c. Spectrogram of the filtered N-S component. The T phase is observed both in the time series and in the spectrogram, where it shows up with a predominant frequency of about 4.75 Hz. Two separate energy packets can be seen. The signal lasts for about 100 s.

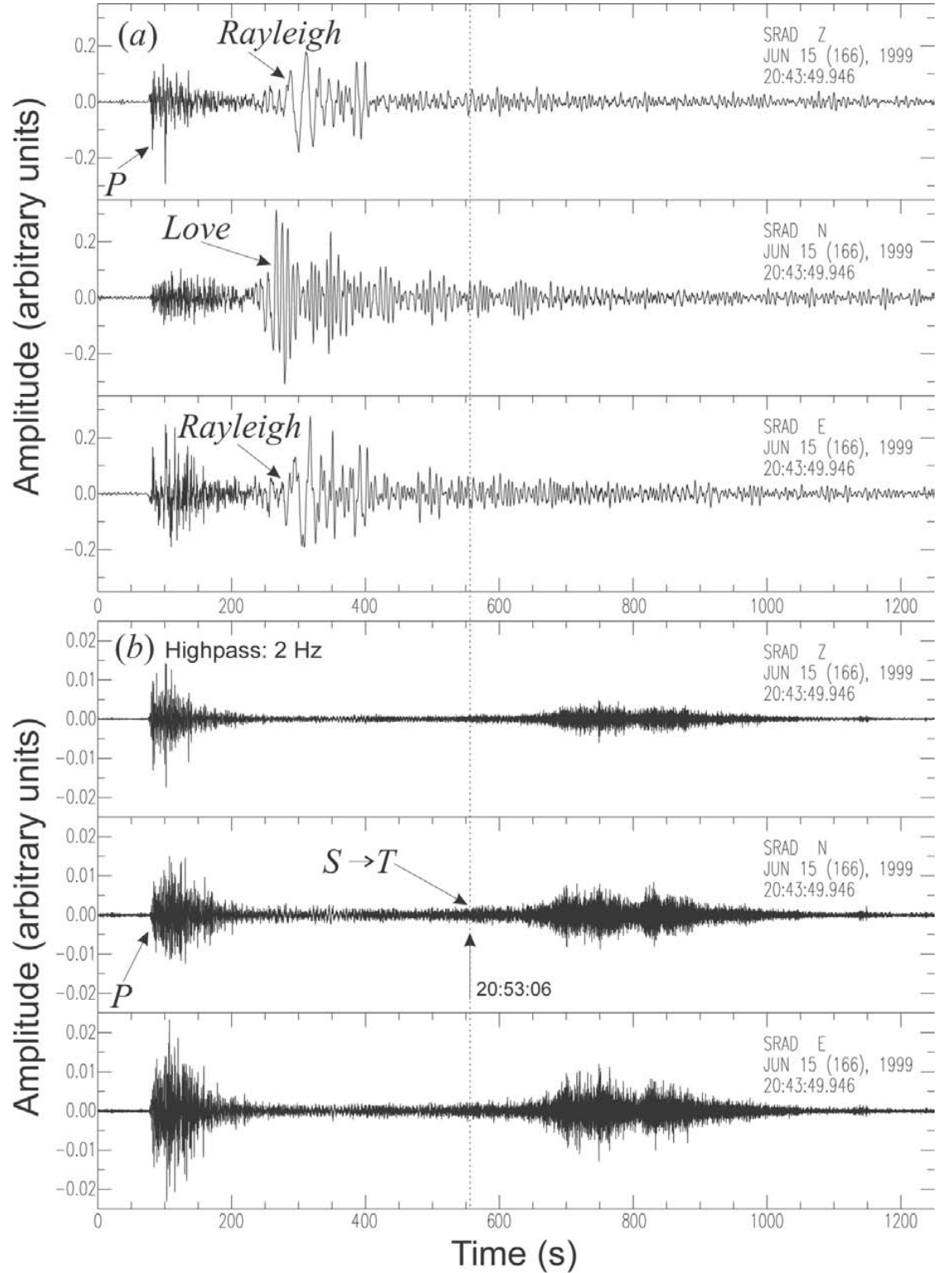


Fig. 4. Velocity records for the Tehuacán earthquake, 06/15/1999, at station SRAD. The station has a backazimuth $\phi_b = 90.7^\circ$. Therefore, the N-S component can essentially be treated as the transverse component. The E-W component is very close to the radial. (a) unfiltered time series for the three components, which are all shown at the same scale. (b) the records were highpass filtered at 2 Hz in order to enhance the T phase. The vertical arrow points to the observed arrival time of the $S \rightarrow T$ wave.

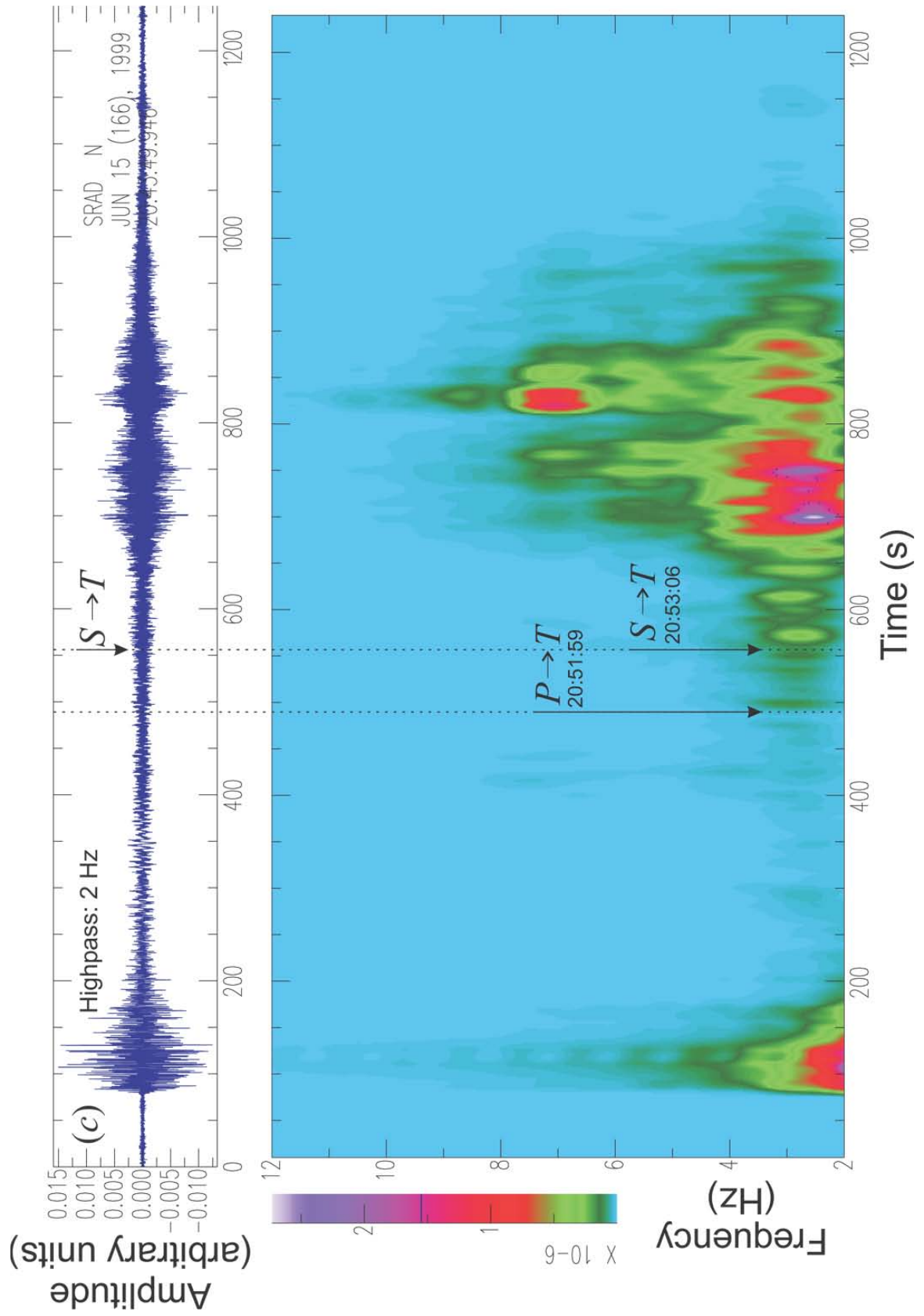


Fig. 4c. Spectrogram of the filtered N-S component. The $P \rightarrow T$ arrival is now visible. The signal lasts for close to 500 s and reaches its maximum amplitude about 200 s after the $P \rightarrow T$ arrival. It has a predominant frequency of about 2.5 Hz.

Okal, 1998) is 494 s. Therefore, the expected arrival times at SRAD are 20:51:47 for the $P \rightarrow T$ wave and 20:52:57 for the $S \rightarrow T$ wave. These calculated arrivals times are 12 s too early relative to the observed arrival time at SRAD for the $P \rightarrow T$ wave (20:51:59), and 9 s too early for the $S \rightarrow T$ wave (20:53:06). Given the uncertainty in reading the observed T arrival times, and also the uncertainty as to the exact location of the seismic-to-acoustic transition point, we feel justified in interpreting the two arrivals in Figure 4c as the $P \rightarrow T$ and the $S \rightarrow T$ waves. Since the S wave carries more energy than the P wave, a greater amplitude should be expected in the $S \rightarrow T$ wave than in the $P \rightarrow T$ wave. This is indeed the case (Figure 4). Since the earthquake occurred inside a subducting slab, it is conceivably possible that the P and S waves travelled up the slab before being converted to T waves. Okal and Talandier (1997, 1998) concluded that the T waves generated by the great 1994 deep Bolivian earthquake could be properly modeled only as involving an $S \rightarrow T$ conversion at the South American shoreline. Furthermore, in order for the S wave to deliver high-frequency energy to the oceanic column requires propagation through a medium with low anelastic attenuation, *i. e.* a thermally and mechanically continuous slab (Okal and Talandier, 1997, 1998). Additionally, Okal and Talandier (1997) explained the arrival time for a T wave recorded on the island of Reao, North Tuamotu group, as the $P \rightarrow T$ conversion from the great Colombian earthquake of July 31, 1970.

The T waves from this event were recorded by all five stations in the experiment (Figure 5a). Thus, it is possible to study the amplitude decay as the distance traveled by the seismic wave in the island is increased. In order to determine the distance traveled from the acoustic-to-seismic conversion point (Table 3), the locations of the stations were plotted on a topographic sheet (Dirección General de Geografía, 1992) and the distances from the stations to the shoreline in the direction of the earthquake were measured. Next the distance from the shoreline to the acoustic-to-seismic transition point in the direction of the source was estimated from the bathymetric map published by Bryan (1966). It was assumed that the transition point is located on the 550-fathom depth contour. This depth is roughly equivalent to 1006 m. The sum of these two distances gives the length of the seismic path through land. The distance increases from 5.1 km at STIR to 10.2 km at SBNA. Figure 5a shows the time domain amplitude decrease of the T phases in the vertical components as the length of the seismic path is increased. The corresponding amplitude spectra are shown in Figure 5b. The frequency-domain amplitudes decay roughly as it would be expected with distance. At a frequency of 2.5 Hz, the amplitude at SBNA drops approximately by a factor of five relative to STIR. Seismograms were highpass filtered at 2 Hz, except for SBNA. The latter was bandpass filtered from 2 to 10 Hz to avoid noise from the power generators nearby.

T phase observations for the event of 06/21/1999 Guerrero state, Mexico.- By the time of this earthquake all stations except SBNA had been dismantled. The three-component seismograms were bandpass filtered between 2 and 10 Hz and show an arrival time for the T wave at about 17:51:59. The total duration of the T wave is close to 250 s as determined from the spectrogram of the filtered N-S component. Since the backazimuth is $\phi_b = 90.3^\circ$, this can be treated as the transverse component. The energy of the T wave is concentrated at frequencies between 2 and 8 Hz with a maximum at about 4.7 Hz.

The travel time for the T wave was calculated from the travel times of a seismic wave propagating through land plus an acoustic wave propagating through water. From a hypsographic map (Dirección General de Geografía, 2000), the location on the continental slope of the seismic-to-acoustic transition point was estimated at 18.6°N , 104.25°W . Thus, the distance from the epicenter to the seismic-to-acoustic conversion point is 2.57° (286 km) and the distance from the transition point to the station is 6.35° (706 km). The travel time for the P wave to the transition point is 40 s and for the S wave is 70 s. For an acoustic wave traveling at 1.48 km/s (Talandier and Okal, 1998), the travel time from the transition point to the station is 477 s. The expected arrival times at SBNA are 17:51:43 for the $P \rightarrow T$ wave and 17:52:13 for the $S \rightarrow T$ wave. The calculated arrival time for the $P \rightarrow T$ wave is 16 s earlier than the observed arrival (17:51:59) while the expected $S \rightarrow T$ arrival is 14 s later than the recorded arrival. The agreement between the observed and the calculated arrival times seems reasonable considering the uncertainty in reading the T arrival times, the uncertainty in the location of the transition point, and the uncertainty in the depth of the earthquake.

T phase observations for the event of 06/23/1999 Rivera Fracture Zone.- This earthquake was recorded by station SBNA, the only one still operational at the end of the experiment. The records for all three components were bandpass filtered between 1 and 10 Hz. The arrival time for the T phase can be seen at about 01:03:04. The duration of the T wave was measured from the spectrogram of the N-S component and is about 70 s. In this case the backazimuth is $\phi_b = 89.7^\circ$. Therefore the N-S component is essentially the same as the transverse. The energy of the T wave is concentrated at frequencies between 1 and 8 Hz with a maximum at about 4.7 Hz.

The epicentral distance is 480 km. Assuming that the whole path were travelled as an acoustic wave at a velocity of 1.48 km/s (Talandier and Okal, 1998), then the expected T arrival time would be 01:03:52. This is 48 s later than the observed arrival time and suggests that a significant portion of the path was traveled as a seismic wave. In order to determine the location of the seismic-to-acoustic conversion point, we looked at a bathymetric map (Dirección General de

Geografía, 1988). There are four seamounts near the epicenter with bathymetric highs ranging between 1876 and 1501 meters below the ocean surface. It is proposed that one of these seamounts is the seismic-to-acoustic transition point. A seismic wave was assumed to propagate between the epicenter and the seamount and its corresponding travel time was calculated. The travel time for the acoustic wave was calculated between the seamount and the station. Two seamounts in particular are likely candidates to serve as the transition point. The first one reaches its highest elevation 1501 m below the ocean surface and is located at 19.0°N, 107.6°W. The distance from the epicenter to this proposed transition point is 1.12° (125 km) with a travel time of 21 s for the P wave and 36 s for the S wave. The distance from the transition point to SBNA is 3.23° (359 km). The travel time for an acoustic wave propagating at 1.48 km/s (Talandier and Okal, 1998) is 243 s. The expected arrival times at the station are 01:02:52 for the $P \rightarrow T$ wave and 01:03:07 for the $S \rightarrow T$ wave. The calculated arrival time for the $P \rightarrow T$ wave is 12 s earlier than the observed arrival (01:03:04) while the expected $S \rightarrow T$ arrival is 3 s later than the recorded arrival. The second seamount has a maximum altitude 1876 m below sea level and is located at 18.7°N, 107.1°W. The distance from the epicenter to the seamount is 0.68° (76 km) while the distance between the seamount and SBNA is 3.63° (404 km). The travel time for the P wave to the transition point is 14 s and for the S wave is 23 s. The travel time for the acoustic wave between the seamount and the station is 273 s. Therefore the arrival times calculated at SBNA are 01:03:15 for the $P \rightarrow T$ wave and 01:03:24 for the $S \rightarrow T$ wave. In this case, the calculated arrival time for the $P \rightarrow T$ wave is 11 s later than the observed arrival (01:03:04) and the expected $S \rightarrow T$ arrival is 20 s later than the recorded

arrival. In both cases the calculated arrival is significantly closer to the observed arrival than if the whole path is assumed to be an acoustic wave propagating through water. While it is not possible to ascertain which seamount acts as the seismic-to-acoustic conversion point, it is expected that the 1501-m seamount would couple the seismic energy more efficiently into the SOFAR channel due to its greater height.

The existence of the Ti phase from earthquakes on the Blanco and Mendocino Fracture Zones has been observed on seismic and hydrophone records at the Hawaii-2 Observatory (H2O), located on the Pacific ocean floor (Butler and Lomnitz, 2002; Lomnitz *et al.*, 2002). This signal propagates along the ocean floor both in the sediments and in the water and travels along a purely oceanic path. Since Ti phases can easily be converted to P waves when they encounter an island or a continental shelf (Lomnitz *et al.*, 2002), it is conceivably possible that the Ti phase from the Rivera FZ earthquake has been recorded by our deployment at Socorro Island.

6. CONCLUSIONS

We installed a total of five portable, temporary seismic stations on Socorro Island in June 1999. The choice of locations was determined by the existence of a dirt road on the southeastern side of the island which made it possible to transport the equipment.

The power spectral density curves for all five stations were calculated. No significant effect from cultural noise was found at the sites surveyed, except for the site at the Navy village (SBNA), where the power generators produce noise at frequencies above 10 Hz. The power spectral densities at each of the five sites remain essentially constant regardless of the time of day, or the day of the week. The small effect of cultural noise on the sites at Socorro Island is due to the low population density, less than 100 persons total. Comparison of the power spectral density curves from all five stations to reference levels for sites around the world shows that Socorro Island is relatively noisy, in agreement with observations at other sites on small islands. The power spectral density curves are similar for the different stations at low frequencies, however, there are clear differences at high frequencies. Stations SRAD and SPAR are the most quiet sites at the frequencies of interest for the detection of earthquake-generated T waves (between 2 and 10 Hz) while STIR is the noisiest.

A total of six seismic events were recorded during the deployment and occurred at distances between 42 and 2202 km. Their magnitudes ranged between 2.8 and 7.0. We recorded one event near the coast of Guatemala; two small, nearby events on the Clarión Fracture Zone; the Tehuacán earthquake of June 15, 1999; one event in Guerrero state; and one earthquake on the Rivera Fracture Zone. The obser-

Table 3

Distances^a from the stations to the acoustic-to-seismic transition point^b Tehuacán earthquake of June 15, 1999

Station	Distance		
	from station to shoreline (km)	from shoreline to 550-fathom contour (km)	from station to 550-fathom contour (km)
STIR	1.50	3.60	5.10
SRAD	1.25	5.00	6.25
SGRU	2.95	3.60	6.55
SPAR	4.05	5.00	9.05
SBNA	2.80	7.40	10.20

^a Stations are arranged in order of increasing distance to transition point

^b The transition point is assumed to be on the 550-fathom contour

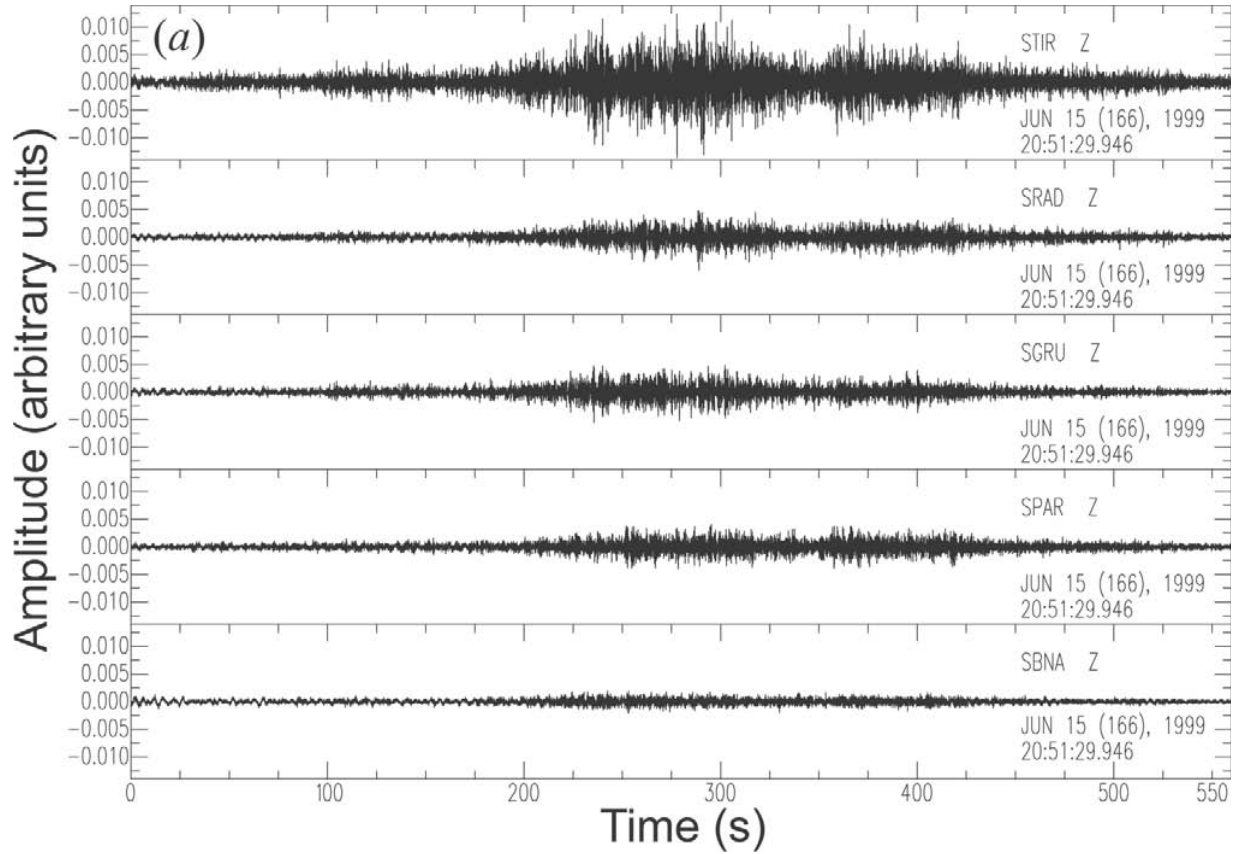


Fig. 5. Vertical component velocity records for the T waves from the Tehuacán earthquake, 06/15/1999. The seismograms are arranged in order of increasing distance traveled by the converted seismic wave through land. All records, except for SBNA, were highpass filtered at 2 Hz. SBNA was bandpass filtered from 2 to 10 Hz to get rid of the noise from the power generators at the navy village. In general the amplitudes decrease with increasing length of the seismic path as expected. (a) time domain records.

vation of earthquakes on the Clarión and Rivera Fracture Zones leads to the expectation that more events will be recorded from several fracture zones in the area once CTBTO's T phase station at Socorro Island becomes operational. Furthermore, the station should also detect the seismic signals from volcanic activity at both Socorro and San Benedicto Islands.

T waves from the four largest and farthest earthquakes were recorded. An event near the coast of Guatemala produced a T wave showing two distinct packets of energy with a combined duration of about 100 s. The second packet shows a greater amplitude than the first one. Both packets have their highest energy at about 4.75 Hz. However, the first packet carries its energy between 3 and 7 Hz while the energy of the second one is concentrated between 2 and 8 Hz. Calculation of the spectrogram for the T phase from an earthquake in Tehuacán shows the arrival of the $P \rightarrow T$ and the $S \rightarrow T$ waves, both with energy between 2 and 3.75 Hz. The total duration of the T phase is close to 500 s and reaches

its maximum amplitude about 200 s after the $P \rightarrow T$ arrival. The T wave contains energy at frequencies between 2 and 10 Hz and reaches its maximum amplitude at about 2.5 Hz. This was an earthquake within the subducted Cocos plate at a depth of 60 km and far from the coast of the Pacific ocean. It is conceivably possible that the seismic P and S waves were channeled up the subducting slab before converting to acoustic energy upon entering the water column at the continental slope. Such channeling was previously reported for the $S \rightarrow T$ wave recorded from the great 1994 deep Bolivian earthquake. An event in Guerrero state produced a T phase lasting almost 250 s. Its energy is concentrated between 2 and 8 Hz and reaches its maximum at about 4.7 Hz. An earthquake in the Rivera Fracture Zone generated a T wave with a duration of about 70 s. The wave carries energy between 1 and 8 Hz with a maximum at about 4.7 Hz. In this case, the source-to-station path is purely oceanic. Thus it is possible that the energy recorded at the island may have propagated as a T_i phase (Butler and Lomnitz, 2002; Lomnitz et al., 2002).

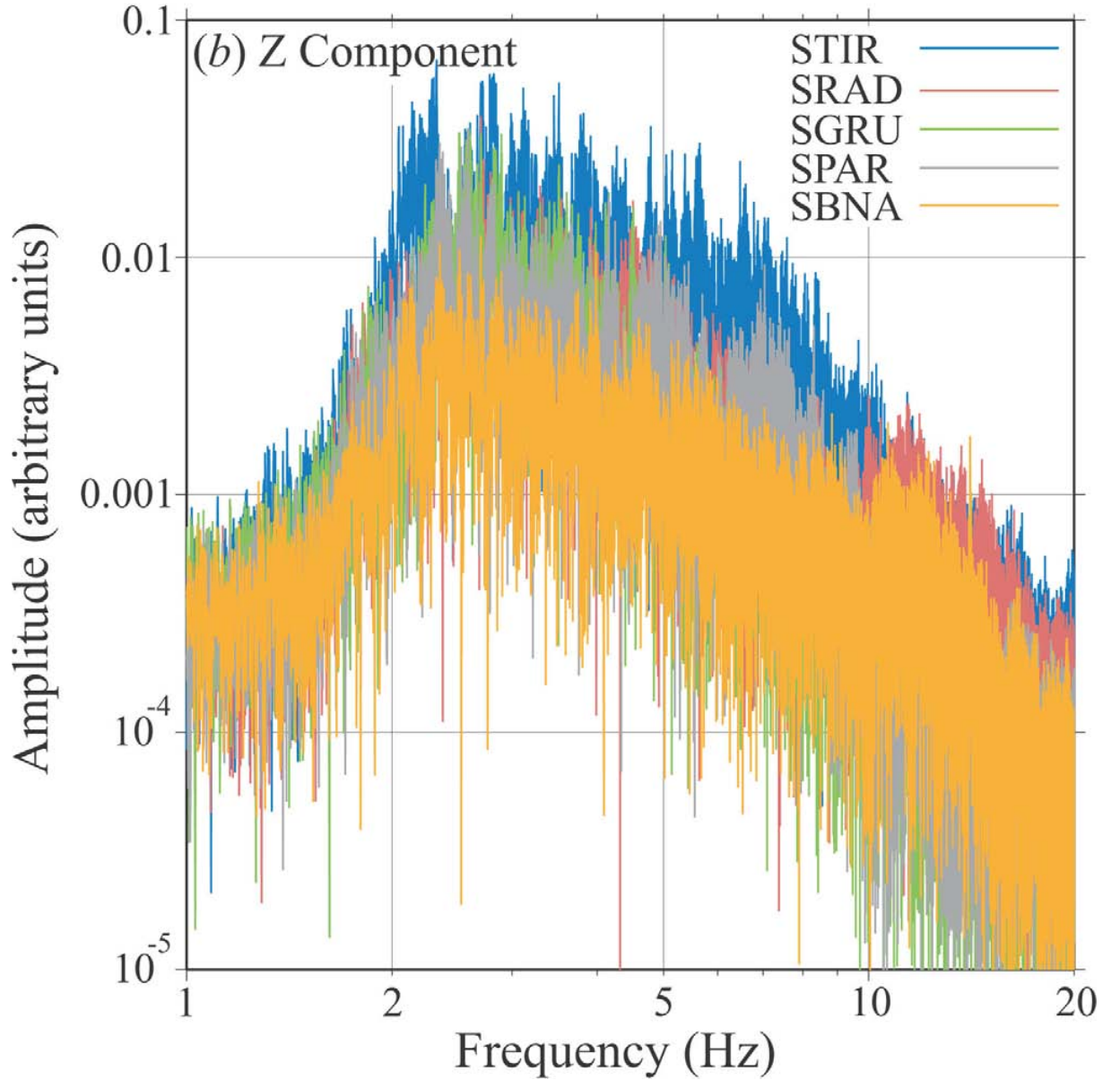


Fig. 5b. Corresponding amplitude spectra.

ACKNOWLEDGMENTS

We are thankful to the Mexican Navy for their valuable assistance making this work possible. We thank the captains and crews of ships Hidalgo and Ortega. We are grateful to Admiral Manuel Eusebio Anguas Mendoza, commander in charge of Socorro Island during our visit. We thank Captain José Benítez Antonio for providing all the necessary personnel, vehicles, and advice, and for his hospitality. We thank the personnel of the Navy stationed at Socorro during our visit. We are also thankful to Captain Salvador Riande Ferreira and Lieutenant Martha Marín Contreras for help with

preparations in Manzanillo. We thank Shri Krishna Singh for his guidance while working on this project. We are grateful to Enrique Guevara, Germán Espitia and Manuel Velázquez for help with preparations for the trip and getting the equipment ready in Mexico City; Enedina Martínez for help with the paperwork for the trip; and Martín Malagón and Víctor Hugo Espíndola for driving to Manzanillo and back. We also thank Carlos Gutiérrez at the Centro Nacional para la Prevención de Desastres for use of seismic equipment. We are grateful to Guillermo González of the Benemérita Universidad Autónoma de Puebla for help with preparations for the trip. We also thank Carlos Mortera for

letting us borrow his laptop computer and for making the trip to the island with us. We are thankful to Luciana Astiz for making her computer program available. Funding for this project was provided by Mexico's Consejo Nacional de Ciencia y Tecnología through grant 36671-T.

BIBLIOGRAPHY

- BRYAN, W. B., 1966. History and mechanism of eruption of soda-rhyolite and alkali basalt, Socorro Island, Mexico. *Bull. Volcanol.*, 29, 453-480.
- BUTLER, R. and C. LOMNITZ, 2002. Coupled seismoacoustic modes on the seafloor. *Geophys. Res. Lett.*, 29, doi:10.1029/2002GL014722.
- DIRECCIÓN GENERAL DE GEOGRAFÍA, 1988. Islas Revillagigedo, Map CB-006, First edition, Second printing, scale 1:1,000,000, Instituto Nacional de Estadística, Geografía e Informática (INEGI), Mexico City, Mexico.
- DIRECCIÓN GENERAL DE GEOGRAFÍA, 1992. Isla Socorro, Carta topográfica, Map E12B61, First edition, First printing, scale 1:50,000, Instituto Nacional de Estadística, Geografía e Informática (INEGI), Aguascalientes City, Mexico.
- DIRECCIÓN GENERAL DE GEOGRAFÍA, 2000. Estados Unidos Mexicanos, Carta hipsográfica en relieve, Second edition, First printing, scale 1:4,000,000, Instituto Nacional de Estadística, Geografía e Informática (INEGI), Aguascalientes City, Mexico.
- INTERNATIONAL SEISMOLOGICAL CENTRE, 1999. *Bull. Internatl. Seis. Cent.*, 36 (6), Thatcham, United Kingdom.
- KENNETT, B. L. N. and E. R. ENGDahl, 1991. Travel times for global earthquake location and phase identification. *Geophys. J. Int.*, 105, 429-465.
- KULHÁNEK, O., 1990. Anatomy of seismograms, Developments in solid Earth Geophysics, Vol. 18. Elsevier Science Publishers, B. V., Amsterdam. The Netherlands, 178 pp.
- LOMNITZ, C., R. BUTLER and O. NOVARO, 2002. Coupled modes at interfaces: A review. *Geofis. Int.*, 41, 77-86.
- NEWTON, J. and M. GALINDO, 2001. Hydroacoustic Monitoring Network. *Sea Technology*, September, 41-47.
- OKAL, E. A., 2001. *T*-phase stations for the International Monitoring System of the Comprehensive Nuclear-Test Ban Treaty: A global perspective. *Seism. Res. Lett.*, 72, 186-196.
- OKAL, E. A. and J. TALANDIER, 1997. *T* waves from the great 1994 Bolivian deep earthquake in relation to channeling of S wave energy up the slab. *J. Geophys. Res.*, 102, 27,421-27,437.
- OKAL, E. A. and J. TALANDIER, 1998. Correction to “*T* waves from the great 1994 Bolivian deep earthquake in relation to channeling of S wave energy up the slab”. *J. Geophys. Res.*, 103, 2793-2794.
- SIEBE, C., J.-C. KOMOROWSKI, C. NAVARRO, J. McHONE, H. DELGADO and A. CORTÉS, 1995. Submarine eruption near Socorro Island, Mexico: Geochemistry and scanning electron microscopy studies of floating scoria and reticulite. *J. Volcanol. Geotherm. Res.*, 68, 239-271.
- SINGH, S. K., M. ORDAZ, J. F. PACHECO, R. QUAAS, L. ALCANTARA, S. ALCOCER, C. GUTIÉRREZ, R. MELI and E. OVANDO, 1999. A preliminary report on the Tehuacán, Mexico earthquake of June 15, 1999 ($M_w=7.0$). *Seism. Res. Lett.*, 70, 489-504.
- SULLIVAN, J. D., 1998. The Comprehensive Test Ban Treaty. *Physics Today*, 51, 3, 24-29.
- TALANDIER, J. and E. A. OKAL, 1979. Human perception of *T* waves: The June 22, 1977 Tonga earthquake felt on Tahiti. *Bull. Seism. Soc. Am.*, 69, 1475-1486.
- TALANDIER, J. and E. A. OKAL, 1998. On the mechanism of conversion of seismic waves to and from *T* waves in the vicinity of island shores. *Bull. Seism. Soc. Am.*, 88, 621-632.

Raúl W. Valenzuela¹, Marta Galindo², Javier F. Pacheco¹, Arturo Iglesias¹, Luis F. Terán¹, José L. Barreda³ and Carlos Coba³

¹ Departamento de Sismología, Instituto de Geofísica, Universidad Nacional Autónoma de México, Circuito de la Investigación S/N, Cd. Universitaria, Del. Coyoacán, 04510 México, D. F., México
Email: raul@ollin.igeofcu.unam.mx

² Hydroacoustic Monitoring Section, International Monitoring System Division, Comprehensive Nuclear-Test-Ban Treaty Organization, Vienna International Centre, P. O. Box 1250, A-1400 Vienna, Austria.

³ Facultad de Ingeniería, Benemérita Universidad Autónoma de Puebla, 4 Sur No. 104, Centro, 72000 Puebla, Pue., México.